

LIMUSE: LIGHTWEIGHT MULTI-MODAL SPEAKER EXTRACTION

Qinghua Liu^{1,2†}, Yating Huang^{1,3†}, Yunzhe Hao^{1,3}, Jiaming Xu^{1,3‡}, Bo Xu^{1,3,‡}

¹Institute of Automation, Chinese Academy of Sciences (CASIA), Beijing, China

²Qiushi Honors College, Tianjin University, Tianjin, China

³School of Future Technology, University of Chinese Academy of Sciences, Beijing, China

tsinghua.liu@tju.edu.cn, {huangyating2016, haoyunzhe2017, jiaming.xu, xubo}@ia.ac.cn

Abstract

In recent years, multi-modal cues, including spatial information, facial expression and voiceprint, are introduced to the speaker extraction task to serve as complementary information to each other to achieve better performance. However, the front-end models, for speaker extraction, become large and hard to deploy on a resource-constrained device. In this paper, we address the aforementioned problem with novel model architectures and model compression techniques, and propose a lightweight multi-modal framework for speaker extraction (dubbed LiMuSE), which adopts Group Communication (GC) to decrease the width of sequence modeling module by splitting high-dimensional features into groups of low-dimensional features which could be run in parallel, and the Context Codec (CC) to decrease the length of sequential feature by compressing temporal context, and further uses an ultra-low bit quantization technology to achieve lower model size. The experiments on the GRID dataset show that incorporating GC and CC into the multi-modal framework achieves on par or better performance with fewer parameters and less model complexity, and further applying the quantization technology obtains about 180 times compression ratio while maintaining a comparable performance compared with baselines. Our code will be available at <https://github.com/aispeech-lab/LiMuSE>.

Index Terms: Lightweight, Speaker Extraction, Multi-Modality, Group Communication, Quantization

1. Introduction

The Cocktail Party effect is a fundamental topic in auditory scene analysis, which refers to the phenomenon that humans are able to focus his/her attention on specific auditory stimuli by masking out the acoustic background noise in complex auditory scenes [1]. With the rapid developments of deep learning technologies, more and more methods have been proposed to solve the task, among which could typically be divided into two types: blind speech separation and speaker extraction.

Blind speech separation aims to mimic the human's bottom-up stimulus-driven attention by simultaneously estimating the speech of different speakers from the mixture, which is often confronted with two problems: permutation problem [2] and output dimension mismatch problem [3]. By contrast, speaker extraction (also termed as target speech separation) only extracts the speech of interest from an overlapped audio of simultaneous speakers. Speaker extraction emulates human's top-down voluntary focus [4] by utilizing information from the target speaker as prior knowledge to direct the attention to the in-

terested speaker. Therefore, speaker extraction avoids the permutation problem and output mismatch problem inherently.

Speaker extraction often requires additional information that identifies the target speaker. Voiceprint, which characterizes a speaker, is proved to be an important cue in auditory scene analysis [5, 4, 6, 7]. Recently, incorporating visual information such as face or lip image sequences, in which phonetic or prosaic content coincides with muscle movements, into speaker extraction systems becomes an emerging research focus to improve the robustness and separation quality [8, 9, 10, 11]. What's more, multi-channel-based methods can extract additional direction features to further improve the performance [12, 13]. By utilizing all the available information of the target speaker mentioned above, Gu et al. [14] demonstrate the effectiveness and steadiness of the multi-channel multi-modal systems. The motivation is that, the acoustic information of the target speaker can be blurry in challenging acoustic environments, while other modalities can provide complementary and steady information to increase the quality. However, the introduction of multi-modal information usually requires more expensive computation cost, which further restricts the deployment of such techniques on resource-constrained platforms, such as mobile phones and other edge devices.

In order to alleviate the deployment problem on resource-constrained devices, there are mainly two types of methods: design of novel model architectures and model compression methods. MobileNetV2 [15] builds a lightweight deep neural network by introducing novel layer modules and changing the internal structure of convolutional blocks. The practice of Group Communication [16] proves that a small, group-shared module is adequate to preserve the model capacity given the inter-group modeling step. Furthermore, Group Communication with Context Codec (GC3) [17] cultivates a more efficient model design to decrease model size without sacrificing performance. Besides, various model compression methods have been proposed to lighten deep neural networks, such as parameter pruning [18, 19], knowledge distillation [20, 21] and quantization [22, 23, 24]. Different from the adjustment of model architectures, the quantization technology compresses a model by converting a full-precision neural network into a low-bitwidth integer version. By limiting the model topology and quantizing the model to 8-bit integer form, VoiceFilter-Lite [5] makes the model tiny and fast to meet strict on-device production requirements.

In this paper, we propose a lightweight multi-modal speaker extraction framework, which incorporates multi-channel information, target speaker's visual feature and voiceprint as reference information and further apply Group Communication, Context Codec and an ultra-low bit quantization technology to reduce the model size and complexity while maintaining relatively high performance. Our contributions can be concluded as

[†]Co-first authors

[‡]Corresponding authors

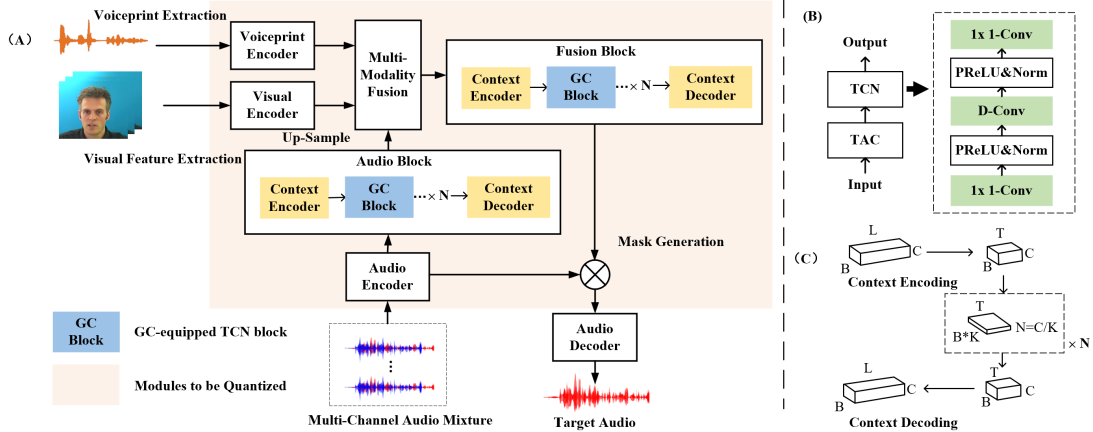


Figure 1: An illustration of LiMuSE framework. (A) The overall architecture of the proposed model and modules to be quantized. ‘GC Block’ indicates the GC-equipped TCN block. (B) Details of GC-equipped TCN block. ‘D-Conv’ indicates a depthwise convolution. (C) Sequence processing pipeline in Audio Block and Fusion Block.

follow:

1. As far as we know, it is the first time that Group Communication has been explored on a multi-modal speaker extraction model. The results have shown the effectiveness, and an appropriate number of groups may promote the inter-modal information exchange and even achieve an improvement;
2. We incorporate GC-equipped TCN block in the process of sequence modeling and Context Codec to decrease both the width of neural network and length of sequential feature without using RNN-related structures, which is more friendly to incorporate quantization technologies, as attempts for quantization of RNNs may show considerable performance degradation with low bit-width weights and activations.
3. We further compress the model size with quantization technologies. The results have shown that our model with ultra-low bit quantization can also maintain a comparable performance, compared with the baselines.

2. Model Design

Our proposed model is a multi-stream architecture that takes multi-channel audio mixture, target speaker’s enrolled utterance and visual sequences of detected faces as inputs, and outputs the target speaker’s mask in the time domain. The encoded audio representations of the mixture are then multiplied by the generated mask to obtain the target audio. Figure 1 provides an overview of our network.

2.1. Audio and Video Representations

2.1.1. Audio Stream

The audio encoder tries to encode mixture speech samples into a spectrum-like frame-based embedding sequence in the latent space, while the decoder is used to transform the masked encoder representation to the target waveform in time domain. Audio encoder and decoder perform the 1-dimensional convolution and deconvolution operation, respectively.

2.1.2. Speaker Embedding Stream

The voiceprint encoder takes the speaker embeddings of the target speaker. We use an off-the-shelf speaker diarization toolkit pyannote [25] to extract the speaker embeddings. The voiceprint encoder is a fully connected layer in this paper. Voiceprint models the characteristics of the target speaker and serves as prior knowledge here to assist the model to filter the speech of target speaker from the mixture.

2.1.3. Video Stream

We obtain face embeddings of the target speaker in videos using the network in [9], which extracts speech-related visual features from visual inputs explicitly by the adversarially disentangled method. The pretrained face embedding extraction network is trained on LRW dataset [26] and MS-Celeb-1M dataset [27].

The visual encoder then maps the extracted face embeddings to match the feature dimension of the encoded audio features. In particular, here we simply use a linear layer after face embedding extraction phase rather than depth-wise separable convolution adopted by AV-ConvTasnet [8] or LSTM [28] adopted by AVMS [11]. Moreover, since the time resolution of video and audio stream is different, we upsample the face embeddings along the temporal dimension to synchronize the audio and video stream by nearest neighbor interpolation. The face embeddings are then used to model the temporal synchronization and interaction between visemes and speech [29].

2.2. Separation Module

2.2.1. GC-Equipped TCN block

In order to reduce the number of parameters, we apply Group Communication (GC) [17] to the separation modules. Given a feature $\mathbf{H} \in \mathbb{R}^N$, it can be decomposed into K groups of low-dimensional feature vectors $\{\mathbf{g}^i\}_{i=1}^K$. A GC module is applied to capture the inter-group dependencies.

We use Transform-Average-Concatenate (TAC) module [30] for the GC module. It is similar to the squeeze-and-excitation design paradigm [31], where there is a residual connection between a pool of features and a global-averaged feature which is generated to summarize the input feature pool. For the specific structure of TAC module, please refer to this arti-

cle [30]. It is demonstrated in [17] that using TAC for the Group Communication module achieves better performance and less calculation cost than other network structure, such as BLSTM and self-attention.

In this paper, Group Communication is applied before each Temporal Convolutional Network (TCN) block [32], which forms GC-equipped TCN block, as is shown in Figure 1 (B). Each TCN block contains a depth-wise separable convolution, PReLU activation [33] and a normalization operation. By introducing Group Communication to TCN block, the model width for TCN block decreases from N to N/K when there is no overlapping within the groups.

2.2.2. Context Codec with GC-Equipped TCN block

It is demonstrated in [34] that speech has a rich temporal structure over multiple time scales, which leads us to think about how to make efficient use of this feature.

In particular, Context Codec [17] is proposed to decrease sequence length as a nonlinear downsampling step by compressing the context of feature vectors into a summary one and then decompress it back to the context. A Context Codec contains a context encoding and decoding module.

Given a sequence of feature \mathbf{H} , the context encoder first splits it along the temporal dimension into blocks $\mathbf{D} \in \mathbb{R}^{C \times L}$ with an overlap ratio of 50%, where C denotes the context size and L denotes the squeezed frame. Then the context encoder applies a GC-equipped TCN network for nonlinear transformation to \mathbf{D} and get $\hat{\mathbf{D}}$. At last, a mean operation is applied on the context dimension of $\hat{\mathbf{D}}$ to produce a sequence of summarization vectors which represent the whole feature sequence. The compressed sequence can then be sent into feature processing module. The context decoder adds the output of feature processing module to each time step in \mathbf{D} and applies another GC-equipped TCN network for the nonlinear transformation. Overlap-add is then applied on it to form the sequence of feature of the original length. The implementation details can be found in our released source code.

2.2.3. Audio Block and Fusion Block

In order to capture the long-term dependencies in the encoded audio features, the audio block is composed of several GC-equipped TCN blocks. In audio block, we use two repeats of TCN blocks, and each repeat of TCN network is composed of several TCN blocks. The dilation factor of depth-wise convolution increases exponentially by two in each repeat, which enlarges the receptive fields of module to capture the correlation in a larger time scale.

The output of the audio block is gathered with the encoded voiceprint and visual features through concatenation. We use a repeat of GC-equipped TCN blocks with exponential increasing dilation factor of depth-wise convolution in fusion block. The voiceprint and visual cues serve as auxiliary information to help the model to extract the target speech from the mixture. A convolutional layer is followed by the fusion block to generate the mask of the target speaker.

2.3. Ultra-low Bit Quantization

2.3.1. Weight Quantization

In this section, we explore quantization function to quantize weights to ultra-low bits. Inspired by [36], the quantization function combines a linear combination of several simple func-

Table 1: Hyperparameters of LiMuSE.

Symbol	Description	Value
N	Number of channels in audio encoder	128
L	Length of the filters (in audio samples)	32
P	Kernel size in convolutional blocks	3
R_a	Number of repeats in audio block	2
R_f	Number of repeats in fusion block	1
C	Context size (in frames)	32
W_q	Weight Quantization bit	3
A_q	Activation Quantization bit	8
T_0	Temperature increment per epoch	5

tions to reformulate the ideal quantization operation and gradually approximates it by controlling the temperature parameter during training. The introduction of temperature parameter narrows the performance gap between the training and inference phase. Starting from a small temperature and gradually increasing it, the quantized neural networks can be well learned.

Suppose that x is the full-precision value to be quantized, y is the quantized integer constrained to a predefined set γ , then the quantization function in the training procedure is formulated as follows:

$$y = Q(x) = \alpha \left(\sum_{i=1}^q s_i \sigma(T(\beta x - b_i)) - o \right), \quad (1)$$

$$\sigma(Tx) = \frac{1}{1 + \exp(-Tx)}, \quad (2)$$

where $q = |\gamma| - 1$, $s_i = \gamma_{i+1} - \gamma_i$, T denotes the temperature parameter. α and β are learnable scale factors of the output and input, respectively. The global offset is defined as $o = \frac{1}{2} \sum_i^n s_i$. Once the target quantization integer set γ is given, $n = |\gamma| - 1$, s_i and the offset o can be directly obtained.

While in the inference phase, we use the ideal quantization function as follows:

$$y = \sum_{i=1}^q s_i A(\beta x - b_i) - o, \quad (3)$$

$$A(x) = \begin{cases} 1 & x \geq 0, \\ 0 & x < 0. \end{cases} \quad (4)$$

In this paper, we perform layer-wise non-uniform quantization, in which weights from different layers use different quantization functions.

2.3.2. Activation Quantization

We also quantize activations of the corresponding quantized layers to make matrix multiplication run faster. For activation quantization, we use the most commonly used 8-bit min-max linear quantization [37]. Straight-Through Estimator (STE) [38] is used to backpropagate the gradients through quantized activations.

2.4. Loss Function

We use Scale-Invariant Signal-to-Distortion ratio (SI-SDR) between predicted wave $\hat{\mathbf{s}}$ and clean wave \mathbf{s} to optimize the network from end to end. The loss function is defined as:

$$\begin{cases} \mathbf{s}_{target} = \frac{\langle \hat{\mathbf{s}}, \mathbf{s} \rangle}{\|\mathbf{s}\|^2} \mathbf{s}; \\ \mathbf{e}_{noise} = \hat{\mathbf{s}} - \mathbf{s}_{target}; \\ SI - SDR(\mathbf{s}_{target}, \mathbf{s}) = 10 \log_{10} \frac{\|\mathbf{s}_{target}\|^2}{\|\mathbf{e}_{noise}\|^2}; \end{cases} \quad (5)$$

Table 2: Performance of LiMuSE under various configurations and comparison with baselines. K stands for number of groups. Q stands for quantization, CC stands for Context Codec, VIS stands for visual cue and VP stands for voiceprint cue. 1ch and 2ch represents single-channel and dual-channel mix speech input stream.

Method	K	SI-SDR	SDR	SDRi	#Params	Model Size	MACs
LiMuSE	32	15.53	16.67	16.46	0.41M	0.19MB (0.56%)	3.98G (7.46%)
	16	17.25	17.71	17.50	1.12M	0.48MB (1.41%)	7.52G (14.1%)
LiMuSE (w/o Q)	32	21.75	22.61	22.40	0.41M	1.55MB (4.54%)	3.98G (7.46%)
	16	24.27	24.83	24.63	1.12M	4.28MB (12.5%)	7.52G (14.1%)
LiMuSE (w/o Q and CC)	32	19.17	20.71	20.50	0.37M	1.40MB (4.1%)	5.94G (11.1%)
	16	23.78	23.65	23.45	0.97M	3.70MB (10.8%)	11.77G (22.1%)
LiMuSE (w/o Q and VP)	32	20.66	21.73	21.53	0.21M	0.81MB (2.37%)	2.25G (4.22%)
	16	21.13	22.38	22.17	0.60M	2.30MB (6.47%)	4.03G (7.56%)
LiMuSE (w/o Q and VIS)	32	14.75	16.32	16.11	0.25M	0.94MB (2.75%)	2.25G (4.22%)
	16	18.57	20.75	20.54	0.63M	2.42MB (7.09%)	4.03G (7.56%)
LiMuSE (raw 2ch)	-	23.54	24.02	23.83	8.95M	34.14MB (100%)	53.34G (100%)
LiMuSE (raw 1ch)	-	12.43	13.37	13.16	8.95M	34.13MB	53.33G
AVMS [11]	-	-	-	15.74	5.80M	22.34MB	60.66G
AVDC [35]	-	-	9.30	8.88	-	-	-
Conv-TasNet [32]	-	14.97	15.48	15.27	3.48M	13.28M	21.44G

3. EXPERIMENT SETTINGS

We evaluate our system on speaker extraction problems using GRID dataset [39], which contains 18 male speakers and 15 female speakers, and each of them has 1,000 frontal 3 second long face video recordings. We randomly select 3 males and 3 females to construct a validation set of 2.5 hours and another 3 males and 3 females for a test set of 2.5 hours. The rest of the speakers form the training set of 30 hours. To construct a 2-speaker mixture, we randomly choose two different speakers and select audio from each chosen speaker, then mix these two clips at a random SNR level between -5 dB and 5 dB. Then we use SMS-WSJ toolkit [40] to obtain simulated anechoic dual-channel audio mixture. We place 2 microphones at the center of the room. The distance between microphones is 7 cm.

We first train the full-precision network for 50 epochs with the initial learning rate set to $1e^{-3}$. Then to train the quantization network, we load the weights of the pretrained full-precision model to get a good starting point. In the quantization stage, the whole separation module and mask generation module are quantized. The weights of encoders are also quantized. The temperature T in quantization function is set to 5 at start and increases linearly with respect to the epochs, which is $T = 5 \times epochs$. The learning rate is halved if the accuracy of validation set has not improved for 4 consecutive epochs. Adam [41] is used as the optimizer. The hyperparameters of the network are shown in Table 1.

4. RESULTS AND DISCUSSIONS

Table 2 presents the performance of LiMuSE under different configurations. We report the SDR, SDRi and SI-SDR score for the evaluation of the model performance. For model complexity, the number of parameters, the model size and the number of MAC operations (MACs) are reported as metrics.

As can be seen from the table, incorporating dual-channel information into LiMuSE (raw 1ch), which includes visual and voiceprint cues while adopts conventional TCN block [32] without GC, CC and Quantization, the performance has been greatly improved. Based on this observation, we conduct following experiments on dual-channel speech stream. After the incorporation of GC and CC, LiMuSE (w/o Q) achieves much smaller

model size and less complexity while maintaining on par or even better performance under a suitable number of groups compared with LiMuSE (raw 2ch) which doesn't adopt proposed lightweight techniques. It suggests that an appropriate number of groups may promote the inter-modal information exchange and achieve improvement. Also, we can learn from the results under different configuration of K (number of groups) that larger K brings about smaller model size with some quality trade-off. The impact of Context Codec, which can be inferred from LiMuSE (w/o Q and CC), could be summarized as reducing model complexity and improving performance while bringing about slight increment of model size.

The ablation study of visual and voiceprint cues demonstrates that the quality decreases after discarding the voiceprint and visual feature respectively, which reveals that they serve as complementary information for each other when both fed into the model. What's more, we can conclude that visual cue is more informative as auxiliary reference than audio cue and suffers less quality loss when we increase the number of groups.

Furthermore, we apply ultra-low bit quantization to compress the model size and achieves as much as 180 times of compression ratio (LiMuSE, $K=32$), which demonstrates that the speaker extraction model can achieve high compression rate. At the same time, it maintains a comparable performance compared with the audio-only baseline (TasNet [32]) and audio-visual baseline (AVMS [11] and AVDC [35]).

5. Conclusion

In this paper, we propose a lightweight multi-modal speaker extraction model incorporating voiceprint and visual feature as complementary cues. We apply Context Codec to decrease the sequence modeling length and Group Communication to achieve smaller model width. Furthermore, we explore the impact of the quantization technology. Compared with original floating-point numbers expressed in 32 bits, in the quantization stage, the weights and activations are quantized to 3 and 8 bits respectively, which significantly decreases model size. Our experiments show that LiMuSE achieves promising results on GRID dataset, and the quantized model achieves comparable performance compared with baselines.

6. References

- [1] A. W. Bronkhorst, “The cocktail party phenomenon: A review of research on speech intelligibility in multiple-talker conditions,” *Acta Acustica united with Acustica*, vol. 86, no. 1, pp. 117–128, 2000.
- [2] D. Yu, M. Kolbæk, Z.-H. Tan, and J. Jensen, “Permutation invariant training of deep models for speaker-independent multi-talker speech separation,” in *ICASSP*. IEEE, 2017, pp. 241–245.
- [3] Z. Chen, Y. Luo, and N. Mesgarani, “Deep attractor network for single-microphone speaker separation,” *ICASSP*, pp. 246–250, 2017.
- [4] C. Xu, W. Rao, E. S. Chng, and H. Li, “Spex: Multi-scale time domain speaker extraction network,” *IEEE/ACM transactions on audio, speech, and language processing*, vol. 28, pp. 1370–1384, 2020.
- [5] Q. Wang, I. L. Moreno, M. Saglam, K. Wilson, A. Chiao, R. Liu, Y. He, W. Li, J. Pelecanos, M. Nika, and A. Gruenstein, “VoiceFilter-Lite: Streaming Targeted Voice Separation for On-Device Speech Recognition,” in *Interspeech*, 2020, pp. 2677–2681.
- [6] M. Ge, C. Xu, L. Wang, E. S. Chng, J. Dang, and H. Li, “Multi-stage speaker extraction with utterance and frame-level reference signals,” in *ICASSP*. IEEE, 2021, pp. 6109–6113.
- [7] Y. Hao, J. Xu, P. Zhang, and B. Xu, “Wase: Learning when to attend for speaker extraction in cocktail party environments,” in *ICASSP*. IEEE, 2021, pp. 6104–6108.
- [8] J. Wu, Y. Xu, S.-X. Zhang, L.-W. Chen, M. Yu, L. Xie, and D. Yu, “Time domain audio visual speech separation,” in *ASRU*. IEEE, 2019, pp. 667–673.
- [9] H. Zhou, Y. Liu, Z. Liu, P. Luo, and X. Wang, “Talking face generation by adversarially disentangled audio-visual representation,” in *AAAI*, 2019.
- [10] A. Ephrat, I. Mosseri, O. Lang, T. Dekel, K. Wilson, A. Hassidim, W. T. Freeman, and M. Rubinstein, “Looking to listen at the cocktail party: a speaker-independent audio-visual model for speech separation,” *TOG*, vol. 37, no. 4, pp. 1–11, 2018.
- [11] P. Zhang, J. Xu, J. Shi, Y. Hao, L. Qin, and B. Xu, “Audio-visual speech separation with visual features enhanced by adversarial training,” in *IJCNN*. IEEE, 2021.
- [12] C. Li, J. Xu, N. Mesgarani, and B. Xu, “Speaker and direction inferred dual-channel speech separation,” in *ICASSP*. IEEE, 2021, pp. 5779–5783.
- [13] G. Li, S. Liang, S. Nie, W. Liu, M. Yu, L. Chen, S. Peng, and C. Li, “Direction-aware speaker beam for multi-channel speaker extraction,” in *Interspeech*, 2019, pp. 2713–2717.
- [14] R. Gu, S.-X. Zhang, Y. Xu, L. Chen, Y. Zou, and D. Yu, “Multi-modal multi-channel target speech separation,” *IEEE Journal of Selected Topics in Signal Processing*, vol. 14, no. 3, pp. 530–541, 2020.
- [15] M. Sandler, A. Howard, M. Zhu, A. Zhmoginov, and L.-C. Chen, “Mobilenetv2: Inverted residuals and linear bottlenecks,” in *CVPR*, 2018, pp. 4510–4520.
- [16] Y. Luo, C. Han, and N. Mesgarani, “Ultra-lightweight speech separation via group communication,” in *ICASSP*. IEEE, 2021, pp. 16–20.
- [17] —, “Group communication with context codec for lightweight source separation,” *IEEE/ACM Transactions on Audio, Speech, and Language Processing*, vol. 29, pp. 1752–1761, 2021.
- [18] J.-H. Luo, J. Wu, and W. Lin, “Thinnet: A filter level pruning method for deep neural network compression,” in *ICCV*, 2017, pp. 5058–5066.
- [19] S. Han, J. Pool, J. Tran, and W. Dally, “Learning both weights and connections for efficient neural network,” *Advances in neural information processing systems*, vol. 28, 2015.
- [20] G. Hinton, O. Vinyals, and J. Dean, “Distilling the knowledge in a neural network,” *stat*, vol. 1050, p. 9, 2015.
- [21] B. Heo, M. Lee, S. Yun, and J. Y. Choi, “Knowledge distillation with adversarial samples supporting decision boundary,” in *AAAI*, vol. 33, no. 01, 2019, pp. 3771–3778.
- [22] M. Rastegari, V. Ordonez, J. Redmon, and A. Farhadi, “Xnornet: Imagenet classification using binary convolutional neural networks,” in *ECCV*. Springer, 2016, pp. 525–542.
- [23] S. Wu, G. Li, F. Chen, and L. Shi, “Training and inference with integers in deep neural networks,” in *ICLR*, 2018.
- [24] S. Zhou, Y. Wu, Z. Ni, X. Zhou, H. Wen, and Y. Zou, “Dorefanet: Training low bitwidth convolutional neural networks with low bitwidth gradients,” *arXiv preprint arXiv:1606.06160*, 2016.
- [25] H. Bredin, R. Yin, J. M. Coria, G. Gelly, P. Korshunov, M. Lavechin, D. Fustes, H. Titeux, W. Bouaziz, and M.-P. Gill, “pyannotate.audio: neural building blocks for speaker diarization,” in *ICASSP*, Barcelona, Spain, May 2020.
- [26] J. S. Chung, A. Senior, O. Vinyals, and A. Zisserman, “Lip reading sentences in the wild,” in *CVPR*, 2017, pp. 3444–3453.
- [27] Y. Guo, L. Zhang, Y. Hu, X. He, and J. Gao, “Ms-celeb-1m: A dataset and benchmark for large-scale face recognition,” in *ECCV*, B. Leibe, J. Matas, N. Sebe, and M. Welling, Eds. Cham: Springer International Publishing, 2016, pp. 87–102.
- [28] Y. Yu, X. Si, C. Hu, and J. Zhang, “A review of recurrent neural networks: Lstm cells and network architectures,” *Neural Computation*, vol. 31, no. 7, pp. 1235–1270, 2019.
- [29] H. L. Bear and R. Harvey, “Phoneme-to-viseme mappings: the good, the bad, and the ugly,” *Speech Communication*, vol. 95, pp. 40–67, 2017.
- [30] Y. Luo, Z. Chen, N. Mesgarani, and T. Yoshioka, “End-to-end microphone permutation and number invariant multi-channel speech separation,” in *ICASSP*. IEEE, 2020, pp. 6394–6398.
- [31] J. Hu, L. Shen, and G. Sun, “Squeeze-and-excitation networks,” in *CVPR*, 2018, pp. 7132–7141.
- [32] Y. Luo and N. Mesgarani, “Conv-tasnet: Surpassing ideal time-frequency magnitude masking for speech separation,” *IEEE/ACM transactions on audio, speech, and language processing*, vol. 27, no. 8, pp. 1256–1266, 2019.
- [33] K. He, X. Zhang, S. Ren, and J. Sun, “Delving deep into rectifiers: Surpassing human-level performance on imagenet classification,” in *ICCV*, 2015, pp. 1026–1034.
- [34] D. T. Toledano, M. P. Fernández-Gallego, and A. Lozano-Diez, “Multi-resolution speech analysis for automatic speech recognition using deep neural networks: Experiments on timit,” *PLoS one*, vol. 13, no. 10, p. e0205355, 2018.
- [35] R. Lu, Z. Duan, and C. Zhang, “Audio-visual deep clustering for speech separation,” *IEEE/ACM Transactions on Audio, Speech, and Language Processing*, vol. 27, no. 11, pp. 1697–1712, 2019.
- [36] J. Yang, X. Shen, J. Xing, X. Tian, H. Li, B. Deng, J. Huang, and X.-s. Hua, “Quantization networks,” in *CVPR*, 2019, pp. 7308–7316.
- [37] R. Krishnamoorthi, “Quantizing deep convolutional networks for efficient inference: A whitepaper,” *arXiv preprint arXiv:1806.08342*, 2018.
- [38] M. Courbariaux, Y. Bengio, and J.-P. David, “Binaryconnect: Training deep neural networks with binary weights during propagations,” *Advances in neural information processing systems*, vol. 28, 2015.
- [39] M. Cooke, J. Barker, S. Cunningham, and X. Shao, “An audio-visual corpus for speech perception and automatic speech recognition,” *The Journal of the Acoustical Society of America*, vol. 120, no. 5, pp. 2421–2424, 2006.
- [40] L. Drude, J. Heitkaemper, C. Boeddeker, and R. Haeb-Umbach, “SMS-WJSJ: Database, performance measures, and baseline recipe for multi-channel source separation and recognition,” *arXiv preprint arXiv:1910.13934*, 2019.
- [41] D. P. Kingma and J. Ba, “Adam: A method for stochastic optimization,” *arXiv preprint arXiv:1412.6980*, 2014.